PHYSICAL REVIEW LETTERS **124,** 077202 (2020)

Exchange Interactions Mediated by Nonmagnetic Cations in Double Perovskites

Vamshi M. Katukuri,[1,*] P. Babkevich,[2,†] O. Mustonen,[3,4] H. C. Walker,[5] B. Fåk,[6] S. Vasala,[7]
M. Karppinen,[3] H. M. Rønnow,[2] and O. V. Yazyev[1]
[1]*Chair of Computational Condensed Matter Physics, Institute of Physics, École Polytechnique Fédérale de Lausanne (EPFL), CH-1015 Lausanne, Switzerland*
[2]*Laboratory for Quantum Magnetism, Institute of Physics, École Polytechnique Fédérale de Lausanne (EPFL), CH-1015 Lausanne, Switzerland*
[3]*Department of Chemistry and Materials Science, Aalto University, FI-00076 Espoo, Finland*
[4]*Department of Material Science and Engineering, University of Sheffield, Mappin Street, Sheffield, S1 3JD, United Kingdom*
[5]*ISIS Neutron and Muon Source, Rutherford Appleton Laboratory, Chilton, Didcot, OX11 OQX, United Kingdom*
[6]*Institut Laue-Langevin, CS 20156, F-38042 Grenoble Cedex 9, France*
[7]*Institut für Materialwissenschaft, Fachgebiet Materialdesign durch Synthese, Technische Universitüt Darmstadt, Alarich-Weiss-Straße 2, 64287 Darmstadt, Germany*

(Received 25 February 2019; revised manuscript received 21 October 2019;
accepted 28 January 2020; published 19 February 2020)

Establishing the physical mechanism governing exchange interactions is fundamental for exploring exotic phases such as quantum spin liquids in real materials. In this Letter, we address exchange interactions in $Sr_2CuTe_xW_{1-x}O_6$, a series of double perovskites that realize a spin-1/2 square lattice and are suggested to harbor a quantum spin liquid ground state arising from the random distribution of nonmagnetic ions. Our *ab initio* multireference configuration interaction calculations show that replacing Te atoms with W atoms changes the dominant couplings from nearest to next-nearest neighbor due to the crucial role of unoccupied states of the nonmagnetic ions in the super-superexchange mechanism. Combined with spin-wave theory simulations, our calculated exchange couplings provide an excellent description of the inelastic neutron scattering spectra of the parent compounds, as well as explaining that the magnetic excitations in $Sr_2CuTe_{0.5}W_{0.5}O_6$ emerge from bond-disordered exchange couplings. Our results demonstrate the crucial role of the nonmagnetic cations in exchange interactions paving the way to further explore quantum spin liquid phases in bond-disordered materials.

DOI: 10.1103/PhysRevLett.124.077202

In $3d$ transition metal (TM) oxides, the on-site Coulomb repulsive interactions between the electrons are strong enough to confine them to the TM sites, leading to the formation of localized spin or spin-orbital moments [1]. The manner in which these moments couple to each other is primarily governed by the underlying exchange interactions, which may be direct and/or mediated by the intermediate anions or ligands (L), the latter is also referred to as the superexchange. There are many possible ways these interactions can manifest, resulting in a plethora of magnetically ordered states such as ferromagnetic and different types of antiferromagnetic (AFM) order, magnetic spirals, or more exotic topologically protected magnetic textures such as Skyrmions [1–4].

Even more fascinating ground states that stem from exchange interactions are those which do not undergo any magnetic ordering even at absolute zero temperature, e.g., spin-liquid states in low-dimensional magnetic systems [5]. Broken-symmetry valence-bond solids and quantum spin liquids (QSLs) where symmetry is conserved are examples of such phases [5–7]. In these quantum paramagnetic phases, the long-range magnetic order is typically destroyed by frustrated exchange interactions and quantum fluctuations [8]. In the simplistic and prototypical two-dimensional spin-1/2 Heisenberg square lattice (HSL) model, the ratio of nearest-neighbor (NN) J_1 and AFM next-nearest neighbor (NNN) J_2 exchange interactions of ∼0.5 results in magnetic frustration and a QSL ground state [7].

The exchange mechanisms in TM compounds, principally the superexchange, are reasonably well understood in the form of the Goodenough-Kanamori-Anderson (GKA) rules [1]. The highly successful GKA rules correctly predict the sign of magnetic coupling for the 180° and 90° TM-L-TM bond angles. In double perovskite compounds like Sr_2CuTeO_6 and Sr_2CuWO_6 the magnetic Cu^{2+} ions are separated by nonmagnetic Te^{6+} and W^{6+} cations, respectively, and the magnetic coupling is a result of the super-superexchange (SSE) mechanism. As shown in Fig. 1, there are multiple SSE paths—the NN exchange is via two identical Cu-O-Te/W-O-Cu paths involving four bridging ligands and two nonmagnetic cations, with a 90° Cu-Te/W-Cu angle. Alternatively, the second or NNN coupling arises from only one Cu-O-Te/W-O-Cu exchange path (180° Cu-Te/W-Cu angle) involving two ligands and a nonmagnetic cation. An interesting aspect in these compounds is whether the nonmagnetic cation participates in the exchange.

In this Letter, we address the following question: do the exchange mechanisms in double perovskite compounds depend on the nonmagnetic cations and, if so, how? We compute the exchange couplings in double perovskite $Sr_2CuTe_xW_{1-x}O_6$ with $x = \{0.0, 0.5, 1.0\}$ compounds using *ab initio* many-body quantum chemistry (QC) calculations. We analyze their microscopic provenance by examining the different SSE paths involved and show that the bridging nonmagnetic cation plays a pivotal role in the exchange mechanism depending on whether it has an empty or completely filled d manifold [9–11]. Further, we decipher the possible physical origin of the features observed in the inelastic neutron scattering (INS) spectrum using spin-wave theory (SWT) while simulating the site disorder phenomena in $Sr_2CuTe_xW_{1-x}O_6$. Our study exposes double perovskites with nonmagnetic cations as the ideal playground to explore bond-disordered couplings and associated QSL phenomena.

The isostructural double perovskite copper oxides Sr_2CuTeO_6 [12] and Sr_2CuWO_6 [13] realize a quasi-two-dimensional spin-1/2 HSL antiferromagnet, despite their three-dimensional crystal structures [14–16]. However, the magnetic order in the two systems is different. While a Néel AFM (NAF) ordering is observed in Sr_2CuTeO_6 with large AFM J_1 and small J_2 of the same sign [15,17], a columnar AFM (CAF) order is stabilized in Sr_2CuWO_6 with small J_1 and large J_2, both AFM [16]. Interestingly, the reported J_2/J_1 ratio in these two compounds differs by two orders of magnitude, 0.03 and 7.92 for Sr_2CuTeO_6 and Sr_2CuWO_6, respectively.

It has been anticipated that a solid solution with equal quantities of Te and W may result in the ratio J_2/J_1 close to 0.5, leading to strong magnetic frustration and possibly producing a spin-liquid ground state [11,18,19]. Interestingly, the macroscopic magnetic features of $Sr_2CuTe_xW_{1-x}O_6$ for $x = 0.5$ show no signs of magnetic ordering, instead indicates its proximity to the highly frustrated $J_2/J_1 = 0.5$ region. Furthermore, the specific heat behavior at low temperatures is reminiscent of a gapless QSL state with collective excitations of entangled spins [11]. Fascinatingly, the suppression of long range magnetic order is observed in a wide region of $x \approx 0.1$–0.6 [20].

Exchange couplings from QC calculations.—Table I compares the Heisenberg exchange couplings defined in Fig. 1 for the end compounds of $Sr_2CuTe_xW_{1-x}O_6$ solid solution—Sr_2CuTeO_6 and Sr_2CuWO_6—obtained from the *ab initio* multireference difference dedicated configuration interaction (MR-DDCI) calculations [21,22]. Those obtained from INS measurements are also shown in the same table. The calculations were done on three different embedded clusters for J_1, J_2, and J_c (see Fig. 1), respectively. For computational details see Ref. [15] and Supplemental Material [23] which includes Refs. [24–39]. In contrast to conventional density functional theory (DFT) and correlated calculations in conjunction with dynamical mean field theory (DFT + DMFT), our calculations are parameter free and accurately describe correlations within the cluster of atoms in a systematic manner. The virtual hopping processes necessary to capture the exchange interactions are well described in this approach, and this makes it the only *ab initio* method that has sufficient predictive capability for estimating magnetic couplings [40–43]. To extract the isotropic exchange couplings, the *ab initio* magnetic spectrum of two unpaired electrons in two Cu^{2+} ions is mapped onto that of a two-spin Heisenberg Hamiltonian $\mathcal{H}_{ij} = J_{ij}\mathbf{S}_i \cdot \mathbf{S}_j$. All calculations were done using the MOLPRO quantum chemistry package [38].

We have previously shown [15] that in Sr_2CuTeO_6 the dominant Heisenberg coupling is the NN AFM J_1, see columns one and two in Table I. The SSE path that gives this large coupling is Cu^{2+}-O^{2-}-O^{2-}-Cu^{2+} along the two bridging TeO_6 octahedra and does not include the Te^{6+} ions explicitly. On the other hand, the NNN J_2 coupling with 180° Cu-Te-Cu angle is significantly smaller and is through the bridging Te atom—Cu^{2+}-O^{2-}-Te^{6+}-O^{2-}-Cu^{2+}.

TABLE I. A comparison of the Heisenberg exchange couplings obtained from *ab initio* MR-DDCI calculations (QC) and experimentally using inelastic neutron scattering (INS) for Sr_2CuTeO_6 [15] and Sr_2CuWO_6 [16]. The couplings obtained from INS are from fits to SWT with a renormalization factor $Z_c = 1.18$ as the first-order correction [44] to calculated magnetic dispersion. All values are given in meV.

	Sr_2CuTeO_6		Sr_2CuWO_6	
	QC	INS [15]	QC	INS [16]
J_1	7.38	7.60(3)	0.68	1.02
J_2	0.05	0.60(3)	8.33	8.50
J_c	0.003	0.04	0.005	⋯

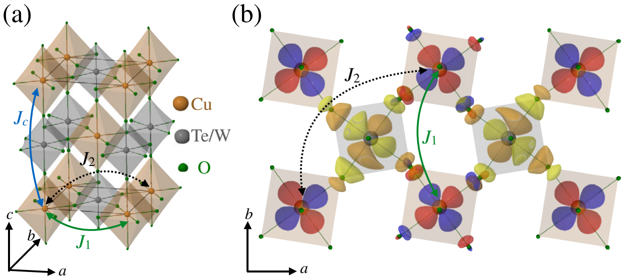

FIG. 1. (a) The crystallographic unit cell of $Sr_2Cu(Te/W)O_6$. (b) The *ab*-plane view of Sr_2CuWO_6 showing the in-plane Cu $3d_{x^2-y^2}$ (red and blue) and W $5d_{x^2-y^2}$ (yellow and orange) orbitals, and the different exchange couplings.

We performed QC calculations for Sr_2CuWO_6 to find a strong NNN J_2 and a small NN J_1 resulting in the ratio $J_2/J_1 \sim 12$. The coupling along the c axis is estimated to be two orders of magnitude smaller, but nevertheless larger than in Sr_2CuTeO_6. These results are consistent with the couplings extracted from the INS data [16]. We note that the magnon-magnon interaction, not included in the linear SWT employed in Ref. [16], could have the same effect as a small NN exchange coupling. Therefore, further corrections to J_1 and J_2 values extracted from the INS might be necessary to account for this. However, we expect this to be small; e.g., in Sr_2CuTeO_6, this corresponds to (J_1, J_2) values being renormalized from (7.60,0.60) to (7.18,0.21) [15].

Given the qualitative similarity of the crystal structures [12,13] as well as the electronic states near the Fermi level [45], it seems surprising to find the dominant ab-plane exchange couplings reversed in the two compounds: J_1 in Sr_2CuTeO_6 and J_2 in Sr_2CuWO_6. It is important to note that the states above (unoccupied) and below (doubly occupied) the Fermi level play an active role in the superexchange process, particularly, if these states belong to the ions bridging the two magnetic sites. In this respect, there is a considerable difference in the unoccupied manifold near the Fermi level in the two compounds. While there is a large density of W $5d$ unoccupied states in Sr_2CuWO_6 at 4 eV above the Fermi level [45], in Sr_2CuTeO_6 the relatively small density of unoccupied states near the Fermi level consists of Te $5p$ character [45]. Further, owing to the delocalized nature of W $5d$ orbitals, there is a considerable dp hybridization with the bridging O $2p$ orbitals leading to appreciable hopping matrix element across the W^{6+} ions. In contrast, the Te $5p$ orbitals are compact and little or zero pp hybridization is expected with O $2p$ orbitals. Thus, in Sr_2CuWO_6 the W^{6+} ions actively participate in the superexchange mechanism.

One might ask "why J_1 is small in Sr_2CuWO_6 ?" given the arguments brought forward in the previous paragraph. To gain more insight into the SSE paths involved in NN and NNN couplings, we have computed J_1 and J_2 by restraining the virtual hopping processes involving the W^{6+} unoccupied orbitals. This can be achieved in QC calculations by setting the coefficients of these orbitals to zero. Although this is unphysical, it gives direct information about the role of W virtual orbitals in the exchange mechanisms.

The NN J_1 coupling along two 90° Cu-W-Cu paths, see Fig. 1(b), decreases to 0.49 meV (~25% reduction) when the unoccupied orbital coefficients of the two W^{6+} ions are eliminated. This implies that the contribution to J_1 from the configurations involving W virtual orbitals is not the leading one. It turns out that the other exchange paths, particularly the Cu-O-O-Cu path, has larger contribution to J_1 just as in the case of Sr_2CuTeO_6 [15]. It should be noted that there are three different W $5d$ orbitals that participate in the SSE mechanism. While the in-plane $5d_{x^2-y^2}$ orbitals, see Fig. 1(b), have σ-overlap with the bridging oxygen $2p$ orbitals and result in an AFM coupling, the out-of-plane degenerate $5d_{xz}$ and $5d_{yz}$ orbitals with π-type overlap contribute to ferromagnetic exchange that is governed by the Hund's rule coupling of the W $5d$ orbitals. A competition of these two mechanisms result in an overall small AFM exchange. On the other hand, constraining the virtual hopping into a single bridging W^{6+} ion's (with 180° Cu-W-Cu angle) unoccupied orbitals results in more than ten times smaller, 0.7 meV, J_2 coupling. This indicates the predominance of the W virtual orbitals in capturing the J_2 coupling. Note that there is only one out-of-plane $5d_{xz/yz}$ orbital participating in the hopping via π overlap which along with σ type hopping through $5d_{x^2-y^2}$ orbital results in an AFM coupling.

We emphasize that in QC calculations all the virtual orbitals of the W^{6+} ions participate in the SSE process and estimating the contributions from a particular virtual orbital is impractical. However, one can understand the SSE from a simplified Hubbard model (SSE-H) that contains two oxygen p orbitals and an additional single W $5d_{x^2-y^2}$ virtual orbital $(d-p-d-p-d)$ compared to a conventional $d-p-d$ model applied for charge-transfer insulators [1]. In Fig. 2, the SSE processes in the J_2 coupling within the SSE-H model are shown. There are three different possible virtual hoppings, represented schematically in Fig. 2, that lift the spin degeneracy and hence contribute to the AFM exchange coupling. In scheme I, Fig. 2(a), the electron from one Cu^{2+} ion can hop to the other and back through the intermediate configurations with a single hole (electron) in O $2p$ (W $5d$) orbitals at a particular instance. This scheme has a dominant contribution to the J_2 coupling. Two other

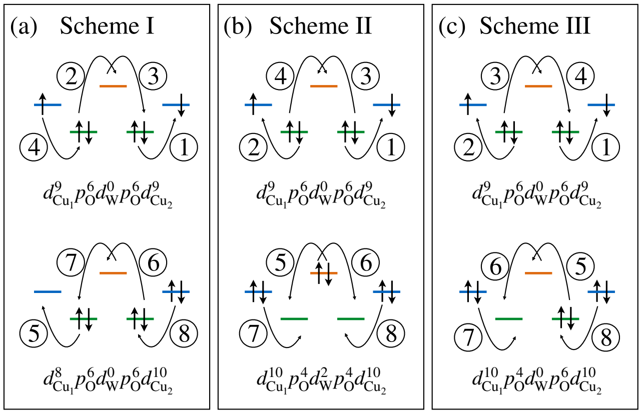

FIG. 2. Super-superexchange mechanisms involved in NNN J_2 coupling in a five band Hubbard model. The three possible intermediate states (see text) that contribute to exchange interaction are shown as three schemes. The Cu $3d_{x^2-y^2}$, O $2p$, and W $5d_{x^2-y^2}$ levels are represented in blue, green, and orange, respectively. The sequence of virtual electron hoppings (arrows) are marked by numbers 1 to 8.

viable possibilities are shown in schemes II and III in Figs. 2(b) and 2(c). Here, configurations where both Cu $d_{x^2-y^2}$ orbitals are doubly occupied are active. While in scheme II both oxygen atoms can contain two holes and the W $5d_{x^2-y^2}$ orbital holds two electrons, in scheme III only one of the oxygen atoms contains two holes. The last scheme contributes twice, as either of the two oxygen atoms can accommodate two holes.

The coupling arising from scheme I can be written as

$$J_2^{\mathrm{I}} = 2\frac{t_{dd}^2}{U_{dd}^{\mathrm{Cu}}}, \quad \text{with} \quad t_{dd} = \frac{t_{pd_{\mathrm{Cu}}}^2}{\Delta_{pd_{\mathrm{Cu}}}} \frac{t_{pd_{\mathrm{W}}}^4}{\Delta_{pd_{\mathrm{W}}}^2}, \qquad (1)$$

where $t_{pd_{\mathrm{Cu}}}$ and $t_{pd_{\mathrm{W}}}$ are the hopping matrix elements from O $2p$ to Cu $3d_{x^2-y^2}$ and from O $2p$ to W $5d_{x^2-y^2}$, respectively, U_{dd}^{Cu} is the on-site Coulomb interaction on the Cu sites, and $\Delta_{pd_{\mathrm{Cu}}}$ and $\Delta_{pd_{\mathrm{W}}}$ are the charge-transfer energies from O $2p$ to Cu $3d$ and W $5d$ orbitals, respectively. Schemes II and III would involve U_{pp}^{O} (U_{dd}^{W}), the Coulomb interactions when two holes (electrons) are accommodated in O $2p$ (W $5d$) orbitals, and yield minor contributions.

Effect of Te/W *atom disorder on the exchange coupling constants.*—Let us consider $\mathrm{Sr_2CuTe_{0.5}W_{0.5}O_6}$ and assume that Te and W atoms are perfectly ordered such that every Cu^{2+} ion is surrounded by two Te^{6+} and two W^{6+} ions. In such a scenario, there are three NN (J_a, J_b, and J_c) and two NNN (J_d and J_e) exchange couplings as show in Fig. 3. Four of the five couplings, J_b, J_c, J_d, and J_e, remain the same as in the end compounds $\mathrm{Sr_2CuWO_6}$ and $\mathrm{Sr_2CuTeO_6}$ as the exchange paths are the same. On the other hand, the exchange channels corresponding to J_a are different compared to the end compounds. We estimated the coupling J_a from our *ab initio* singlet-triplet energy separation for two Cu^{2+} ions with the neighboring environment as shown in Fig. 3. We find this coupling AFM with a magnitude, 0.3 meV, much smaller than the dominant coupling in the end compounds. To summarize, our calculations show that the average J_1 and J_2 can be tuned from effectively 0 to 8 meV through substitution of Te for W, opening up an interesting arena to explore bond disorder of a spin-1/2 square lattice antiferromagnet.

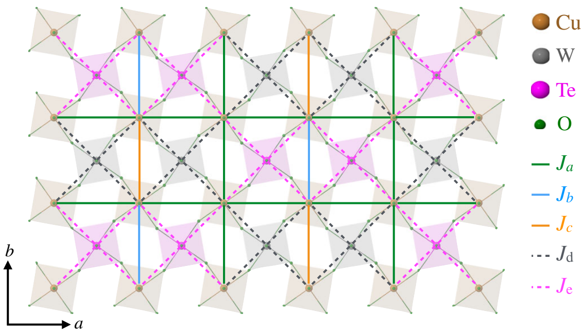

FIG. 3. Square lattice scheme with bond disorder and different possible exchange interactions in $\mathrm{Sr_2CuTe_{0.5}W_{0.5}O_6}$.

INS experiments and SWT calculations.—Measurements on $\mathrm{Sr_2CuTeO_6}$ were performed using the IN4 spectrometer at the ILL utilizing an incident neutron energy of $E_i = 25.2$ meV [46]. The $\mathrm{Sr_2CuTe_xW_{1-x}O_6}$ for $x = 0.5$ and 1.0 samples were studied using MERLIN at ISIS with $E_i = 45$ meV [47]. Further details on $\mathrm{Sr_2CuTeO_6}$ and $\mathrm{Sr_2CuWO_6}$ INS measurements are reported elsewhere [15,16].

Figure 4 shows the inelastic neutron scattering spectra of powder $\mathrm{Sr_2CuTe_xW_{1-x}O_6}$ that have been collected on $x = \{0, 0.5, 1.0\}$ compounds. A background, adjusted for the Bose thermal population factor, recorded at > 100 K has been subtracted from the spectra to remove the phonon contribution at larger $|\mathbf{Q}|$. The end compounds $\mathrm{Sr_2CuWO_6}$ and $\mathrm{Sr_2CuTeO_6}$ show spin waves dispersing from the CAF and NAF zone centers, respectively. A strong band of scattering around 15–17 meV is found in both compounds. This corresponds to a van Hove singularity from the top of the spin-wave dispersion. The INS spectrum of the intermediate $\mathrm{Sr_2CuTe_{0.5}W_{0.5}O_6}$ compound is dramatically different. There appears to be a significant smearing of the spectrum in momentum and energy transfer. The band of scattering corresponding to the van Hove singularity is absent. Weak excitations are observed up to around 20 meV. This scattering decreases with increasing $|\mathbf{Q}|$, as would be expected for magnetic scattering. Magnetic modes emerge from $|\mathbf{Q}| = 0.65$ and 1.4 Å^{-1}, much like in $\mathrm{Sr_2CuWO_6}$, which would suggest the dominant interactions in $\mathrm{Sr_2CuWO_6}$ persist in the $x = 0.5$ compound.

To simulate the INS spectra, we need to construct an appropriate magnetic ground state from which magnetic fluctuations can be calculated. We define a 10×10 square lattice with randomly populated W and Te atoms. The strengths of the $J_1 - J_2$ exchange parameters are as given in Table I and the different possible exchange pathways in the mixed $x = 0.5$ compound are according to Fig. 3. Therefore, J_1 can take values of 7.60 or 1.02 meV depending on whether two Te or W atoms are involved in the exchange process with similar arguments applying to J_2. In the case of one W and one Te atom, we take $J_1 = 0$. From this construction, we find the classical spin configuration which minimizes the total energy and calculate the spin-wave dispersion. To account for truncation of the spin Hamiltonian at the quadratic terms when calculating the one-magnon energy, we rescale the magnon energy by a constant factor of $Z_c = 1.18$ [44]. The calculation is repeated with different distributions of Te and W and the resulting spin-wave pattern is averaged. Figures 4(d)–4(f) show the calculated powder averaged spectra for each composition. Comparing the calculated spectra for $x = 0.5$ to the end compounds, we observe that the simulation predicts a rather broad spectrum. The intense and sharp

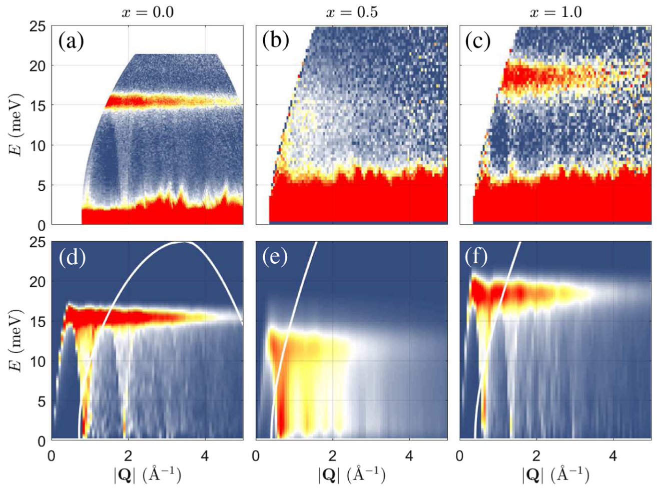

FIG. 4. (a)–(c) Measured inelastic powder spectrum $\chi''(|\mathbf{Q}|, E)$ of $Sr_2CuTe_xW_{1-x}O_6$ for $x = \{0.0, 0.5, 1.0\}$ compositions. The spectra were normalized by nuclear Bragg scattering for easier comparison. In panels (d)–(f) we present the simulations based on a random exchange-bond order. An energy broadening approximating the instrumental resolution has been applied to each calculated spectra. Solid curves in the simulations represent the range of the detector coverage in the corresponding experiment.

scattering at the top of the bandwidth in Sr_2CuWO_6 and Sr_2CuTeO_6 is no longer present for the intermediate compound. Therefore, the effect of the substitution for the intermediate compounds is to leave the powder spectrum featureless with the exception of excitations that emerge from Néel-like and CAF-like low-energy excitations centered at $|\mathbf{Q}| \approx 0.7$ and 1.4 Å^{-1}, respectively. The spectrum, despite the lack of long range magnetic order and contrary to expectations of the limitations of LSWT [48], appears to be in good agreement with the measured powder spectrum, indicating that the bond-disordered exchange couplings reproduce the INS spectrum of $Sr_2CuTe_{0.5}W_{0.5}O_6$.

To summarize, we have computed the NN and NNN Heisenberg exchange couplings in Sr_2CuWO_6 and $Sr_2CuTe_{0.5}W_{0.5}O_6$ finding excellent agreement with available experimental observations. We established that the nonmagnetic cation bridging the magnetic sites play a significant role in the SSE process. In the case of a completely filled d-manifold (Te^{6+}) cation, the exchange path does not include any of its orbitals, but for the d^0 (W^{6+}) bridging cation, the SSE process via these empty orbitals is pivotal. While these conclusions corroborate with DFT + U based studies [16,45,49], it is important to know that the computed exchange couplings strongly depend on the choice of the Coulomb repulsion parameter U. We further provided the rationale for the observed exchange interactions, justifying with numerical evidence. Our simulated INS spectra for Sr_2CuTeO_6 and Sr_2CuWO_6 compare extremely well with experimental data, and they give a good understanding of the measured powder spectrum for $Sr_2CuTe_{0.5}W_{0.5}O_6$. Although further neutron scattering studies are necessary to examine the latter compound, our calculations provide a deep insight into the nature of the interactions within the complex ground state of this system. Our work thus establishes the theoretical background for describing bond-disorder exchange couplings, highlighting site-disordered materials as a new playground for exploring QSL states.

V. M. K. and O. V. Y. acknowledge the support from ERC project “TopoMat” (Grant No. 306504), Swiss NSF NCCR MARVEL and SNSF Sinergia Grant No. CRSII5_171003. The authors would like to acknowledge Swiss National Supercomputing Center (CSCS) under Project No. s832 and EPFL-SCITAS for providing the computational resources.

[*] vamshi.katukuri@epfl.ch
[†] peter.babkevich@epfl.ch

[1] D. Khomskii, *Transition Metal Compounds* (Cambridge University Press, Cambridge, England, 2014).

[2] Y. A. Izyumov, Modulated, or long-periodic, magnetic structures of crystals, Sov. Phys. Usp. **27**, 845 (1984).

[3] U. K. Rößler, A. N. Bogdanov, and C. Pfleiderer, Spontaneous Skyrmion ground states in magnetic metals, Nature (London) **442**, 797 (2006).

[4] S. Mühlbauer, B. Binz, F. Jonietz, C. Pfleiderer, A. Rosch, A. Neubauer, R. Georgii, and P. Böni, Skyrmion lattice in a chiral magnet, Science **323**, 915 (2009).

[5] L. Balents, Spin liquids in frustrated magnets, Nature (London) **464**, 199 (2010).

[6] P. W. Anderson, Resonating valence bonds: A new kind of insulator?, Mater. Res. Bull. **8**, 153 (1973).

[7] P. W. Anderson, The resonating valence bond state in La_2CuO_4 and superconductivity, Science **235**, 1196 (1987).

[8] *Introduction to Frustrated Magnetism: Materials, Experiments, Theory* Springer Series in Solid-State Sciences, edited by C. Lacroix, P. Mendels, and F. Mila, 1st ed. (Springer, Berlin, Heidelberg, 2011).

[9] M. Zhu, D. Do, C. R. Dela Cruz, Z. Dun, H. D. Zhou, S. D. Mahanti, and X. Ke, Tuning the Magnetic Exchange via a Control of Orbital Hybridization in $Cr_2(Te_{1-x}W_x)O_6$, Phys. Rev. Lett. **113**, 076406 (2014).

[10] M. Zhu, D. Do, C. R. Dela Cruz, Z. Dun, J.-G. Cheng, H. Goto, Y. Uwatoko, T. Zou, H. D. Zhou, S. D. Mahanti, and X. Ke, Ferromagnetic superexchange in insulating Cr_2MoO_6 by controlling orbital hybridization, Phys. Rev. B **92**, 094419 (2015).

[11] O. Mustonen, S. Vasala, E. Sadrollahi, K. P. Schmidt, C. Baines, H. C. Walker, I. Terasaki, F. J. Litterst, E. Baggio-Saitovitch, and M. Karppinen, Spin-liquid-like state in a spin-1/2 square-lattice antiferromagnet perovskite induced by $d^{10} - d^0$ cation mixing, Nat. Commun. **9**, 1085 (2018).

[12] D. Reinen and H. Weitzel, Die Kristallstrukturen Cu^{2+}-haltiger oxidischer Elpasolithe Neutronenbeugungsuntersuchungen an den Kristallpulvern, Z. Anorg. Allg. Chem. **424**, 31 (1976).

[13] S. Vasala, J. G. Cheng, H. Yamauchi, J. B. Goodenough, and M. Karppinen, Synthesis and Characterization of $Sr_2Cu(W_{1-x}Mo_x)O_6$: A Quasi-Two-Dimensional Magnetic System, Chem. Mater. **24**, 2764 (2012).

[14] T. Koga, N. Kurita, and H. Tanaka, Strong Suppression of Magnetic Ordering in an $S = 1/2$ Square-Lattice Heisenberg Antiferromagnet Sr_2CuTeO_6, J. Phys. Soc. Jpn. **83**, 115001 (2014).

[15] P. Babkevich, V. M. Katukuri, B. Fåk, S. Rols, T. Fennell, D. Pajić, H. Tanaka, T. Pardini, R. R. P. Singh, A. Mitrushchenkov, O. V. Yazyev, and H. M. Rønnow, Magnetic Excitations and Electronic Interactions in Sr_2CuTeO_6: A Spin-1/2 Square Lattice Heisenberg Antiferromagnet, Phys. Rev. Lett. **117**, 237203 (2016).

[16] H. C. Walker, O. Mustonen, S. Vasala, D. J. Voneshen, M. D. Le, D. T. Adroja, and M. Karppinen, Spin wave excitations in the tetragonal double perovskite Sr_2CuWO_6, Phys. Rev. B **94**, 064411 (2016).

[17] T. Koga, N. Kurita, M. Avdeev, S. Danilkin, T. J. Sato, and H. Tanaka, Magnetic structure of the $S = \frac{1}{2}$ quasi-two-dimensional square-lattice Heisenberg antiferromagnet Sr_2CuTeO_6, Phys. Rev. B **93**, 054426 (2016).

[18] M. Watanabe, N. Kurita, H. Tanaka, W. Ueno, K. Matsui, and T. Goto, Valence-bond-glass state with a singlet gap in the spin-$\frac{1}{2}$ square-lattice random $J_1 - J_2$ Heisenberg antiferromagnet $Sr_2CuTe_{1-x}W_xO_6$, Phys. Rev. B **98**, 054422 (2018).

[19] K. Uematsu and H. Kawamura, Randomness-induced quantum spin liquid behavior in the $s = \frac{1}{2}$ random $J_1 - J_2$ Heisenberg antiferromagnet on the square lattice, Phys. Rev. B **98**, 134427 (2018).

[20] O. Mustonen, S. Vasala, K. P. Schmidt, E. Sadrollahi, H. C. Walker, I. Terasaki, F. J. Litterst, E. Baggio-Saitovitch, and M. Karppinen, Tuning the $s = 1/2$ square-lattice antiferromagnet $Sr_2Cu(Te_{1-x}W_x)O_6$ from Néel order to quantum disorder to columnar order, Phys. Rev. B **98**, 064411 (2018).

[21] J. Miralles, J.-P. Daudey, and R. Caballol, Variational calculation of small energy differences. The singlet-triplet gap in $[Cu_2Cl_6]^{2-}$, Chem. Phys. Lett. **198**, 555 (1992).

[22] J. Miralles, O. Castell, R. Caballol, and J.-P. Malrieu, Specific CI calculation of energy differences: Transition energies and bond energies, Chem. Phys. **172**, 33 (1993).

[23] See the Supplemental Material at http://link.aps.org/supplemental/10.1103/PhysRevLett.124.077202, which contains the computational details.

[24] R. Broer, L. Hozoi, and W. C. Nieuwpoort, Non-orthogonal approaches to the study of magnetic interactions, Mol. Phys. **101**, 233 (2003).

[25] M. Klintenberg, S. Derenzo, and M. Weber, Accurate crystal fields for embedded cluster calculations, Comput. Phys. Commun. **131**, 120 (2000).

[26] D. Figgen, G. Rauhut, M. Dolg, and H. Stoll, Energy-consistent pseudopotentials for group 11 and 12 atoms: Adjustment to multi-configuration Dirac-Hartree-Fock data, Chem. Phys. **311**, 227 (2005).

[27] K. A. Peterson and C. Puzzarini, Systematically convergent basis sets for transition metals. II. Pseudopotential-based correlation consistent basis sets for the group 11 (Cu, Ag, Au) and 12 (Zn, Cd, Hg) elements, Theor. Chem. Acc. **114**, 283 (2005).

[28] T. H. Dunning, Gaussian basis sets for use in correlated molecular calculations. I. The atoms boron through neon and hydrogen, J. Chem. Phys. **90**, 1007 (1989).

[29] D. Andrae, U. Häußermann, M. Dolg, H. Stoll, and H. Preuß, Energy-adjusted *ab initio* pseudopotentials for the second and third row transition elements, Theor. Chim. Acta **77**, 123 (1990).

[30] J. M. L. Martin and A. Sundermann, Correlation consistent valence basis sets for use with the Stuttgart-Dresden-Bonn relativistic effective core potentials: The atoms Ga-Kr and In-Xe, J. Chem. Phys. **114**, 3408 (2001).

[31] R. B. Ross, J. M. Powers, T. Atashroo, W. C. Ermler, L. A. LaJohn, and P. A. Christiansen, *Ab initio* relativistic effective potentials with spinorbit operators. IV. Cs through Rn, J. Chem. Phys. **93**, 6654 (1990).

[32] P.-O. W. K. Pierloot, B. Dumez, and B. O. Roos, Density matrix averaged atomic natural orbital (ANO) basis sets for correlated molecular wave functions, Theor. Chim. Acta **90**, 87 (1995).

[33] K. Fink, R. Fink, and V. Staemmler, *Ab initio* calculation of the magnetic exchange coupling in linear oxo-bridged binuclear complexes of titanium(III), vanadium(III), and chromium(III), Inorg. Chem. **33**, 6219 (1994).

[34] C. J. Calzado, S. Evangelisti, and D. Maynau, Local orbitals for the truncation of inactive space: Application to magnetic systems, J. Phys. Chem. A **107**, 7581 (2003).

[35] A. B. van Oosten, R. Broer, and W. C. Nieuwpoort, Heisenberg exchange enhancement by orbital relaxation in cuprate compounds, Chem. Phys. Lett. **257**, 207 (1996).

[36] N. A. Bogdanov, V. M. Katukuri, H. Stoll, J. van den Brink, and L. Hozoi, Post-perovskite $CaIrO_3$: A $j = 1/2$ quasi-one-dimensional antiferromagnet, Phys. Rev. B **85**, 235147 (2012).

[37] J. Pipek and P. G. Mezey, A fast intrinsic localization procedure applicable for ab initio and semiempirical linear combination of atomic orbital wave functions, J. Chem. Phys. **90**, 4916 (1989).

[38] H. J. Werner, P. J. Knowles, G. Knizia, F. R. Manby, and M. Schütz, Molpro: A general-purpose quantum chemistry program package, Wiley Rev. Comput. Mol. Sci. **2**, 242 (2012).

[39] R. J. Cave and E. R. Davidson, Quasidegenerate variational perturbation theory and the calculation of firstorder properties from variational perturbation theory wave functions, J. Chem. Phys. **89**, 6798 (1988).

[40] R. Maurice, A.-M. Pradipto, C. de Graaf, and R. Broer, Magnetic interactions in $LiCu_2O_2$: Single-chain versus double-chain models, Phys. Rev. B **86**, 024411 (2012).

[41] V. M. Katukuri, H. Stoll, J. van den Brink, and L. Hozoi, *Ab initio* determination of excitation energies and magnetic couplings in correlated quasi-two-dimensional iridates, Phys. Rev. B **85**, 220402(R) (2012).

[42] V. M. Katukuri, S. Nishimoto, V. Yushankhai, A. Stoyanova, H. Kandpal, S. K. Choi, R. Coldea, I. Rousochatzakis, L. Hozoi, and J. van den Brink, Kitaev interactions between $j = 1/2$ moments in honeycomb Na_2IrO_3 are large and ferromagnetic: Insights from *ab initio* quantum chemistry calculations, New J. Phys. **16**, 013056 (2014).

[43] V. M. Katukuri, V. Yushankhai, L. Siurakshina, J. van den Brink, L. Hozoi, and I. Rousochatzakis, Mechanism of Basal-Plane Antiferromagnetism in the Spin-Orbit Driven Iridate Ba_2IrO_4, Phys. Rev. X **4**, 021051 (2014).

[44] R. R. P. Singh, Thermodynamic parameters of the $T = 0$, spin-$1/2$ square-lattice heisenberg antiferromagnet, Phys. Rev. B **39**, 9760 (1989).

[45] Y. Xu, S. Liu, N. Qu, Y. Cui, Q. Gao, R. Chen, J. Wang, F. Gao, and X. Hao, Comparative description of magnetic interactions in Sr_2CuTeO_6 and Sr_2CuWO_6, J. Phys. Condens. Matter **29**, 105801 (2017).

[46] G. Cicognani, H. Mutka, and F. Sacchetti, The thermal neutron time-of-flight spectrometer IN4C, Physica B Condens. Matter **276–278**, 83 (2000).

[47] R. I. Bewley, R. S. Eccleston, K. A. McEwen, S. M. Hayden, M. T. Dove, S. M. Bennington, J. R. Treadgold, and R. L. S. Coleman, MERLIN, a new high count rate spectrometer at ISIS, Physica B Condens. Matter **385–386**, 1029 (2006).

[48] S. Zhang, H. J. Changlani, K. W. Plumb, O. Tchernyshyov, and R. Moessner, Dynamical Structure Factor of the Three-Dimensional Quantum Spin Liquid Candidate $NaCaNi_2F_7$, Phys. Rev. Lett. **122**, 167203 (2019).

[49] S. Vasala, H. Saadaoui, E. Morenzoni, O. Chmaissem, T.-S. Chan, J.-M. Chen, Y.-Y. Hsu, H. Yamauchi, and M. Karppinen, Characterization of magnetic properties of Sr_2CuWO_6 and Sr_2CuMoO_6, Phys. Rev. B **89**, 134419 (2014).